Research Article

Environmental Chemistry and Safety
DOI: 10.26599/ECS.2026.9600030
2026, 2, 9600030

Product characterization and sulfur transformation from waste tires valorization via fast pyrolysis in the presence of hydrogen

Fanfan Xu[1,2†], Yihe Shao[1,6†], Yanpeng Zhang[1,4,5], Bo Wang[3], Peijie Zong[1,4,5], Alar Konist[2], Yuanyu Tian[1,4,5], Jingxian Wang[1,4,5], and Yingyun Qiao[1,4,5*]

[1]State Key Laboratory of Heavy Oil Processing, China University of Petroleum (East China), Qingdao 266580, China

[2]Department of Energy Technology, Tallinn University of Technology, Tallinn 19086, Estonia

[3]Sinopec Dalian Research Institute of Petroleum and Petrochemicals, China Petrochemical Corporation, Dalian 116045, China

[4]Shandong Engineering and Technology Research Center of High Carbon Low Carbonization, China University of Petroleum (East China), Qingdao 266580, China

[5]Qingdao Key Laboratory of Biological Carbon Fixation and Refining, China University of Petroleum (East China), Qingdao 266580, China

[6]Jiaozhou Emergency Management Bureau, Jiaozhou 266300, China

Abstract: Fast pyrolysis in the presence of hydrogen is an advanced thermal decomposition process that enables the conversion of waste tires into value-added products while promoting sulfur transfer. In this study, waste tire pyrolysis experiments were performed in a laboratory-scale downdraft tubular reactor under varying hydrogen concentrations (0–15 vol.%) in the carrier gas. The mass balance of the three-phase products demonstrated an increased yield of gaseous products with hydrogen participation. A partial hydrogen proportion (5 vol.%) slightly enhanced the yield of tire pyrolysis oil (TPO) from 44.25 wt.% to 46.21 wt.%. However, further increases in hydrogen content led to a pronounced reduction in TPO yield, with a significant increase in gaseous products. The chemical composition of TPO was characterized using Fourier transform infrared spectroscopy (FTIR) and gas chromatography–mass spectrometry (GC–MS). The results revealed an increasing proportion of diolefins, predominantly *d*-limonene, accompanied by a decrease in aromatic compounds as the hydrogen concentration increased. Furthermore, iodometric titration, GC–MS, and X-ray photoelectron spectroscopy (XPS) were employed to quantify sulfur-containing species in the gaseous, liquid, and solid products. The findings indicate that hydrogen addition promotes the preliminary desulfurization of TPO and enhances the decomposition of organic sulfur species in pyrolysis carbon black (PCB). The interaction between sulfur radicals and hydrogen radicals facilitates the formation and release of H_2S, thereby promoting sulfur migration from condensed phases to the gas phase.

Key words: Pyrolysis; Hydrogen; Tire pyrolysis oil; Downdraft tube reactor; Product characterization; Sulfur transformation

Citation: Xu F F, Shao Y H, Zhang Y P, et al. Product characterization and sulfur transformation from waste tires valorization via fast pyrolysis in the presence of hydrogen. *Environmental Chemistry and Safety*, 2026, 2, 9600030. https://doi.org/10.26599/ECS.2026.9600030

1. Introduction

The rapid expansion of global vehicle manufacturing and industrial activities has resulted in a substantial increase in the generation of waste tires, posing significant environmental, economic, and logistical challenges [1]. Waste tires are primarily composed of natural and synthetic rubber, carbon black, steel wire, textile fibers, and various chemical additives (e.g., accelerators and antiozonants), rendering them polymeric materials with considerable resource recovery potential [2]. Conventional disposal methods, such as landfilling and incineration, are becoming increasingly unsustainable due to diminishing landfill capacity and increasingly stringent environmental regulations. Consequently, environmentally friendly approaches, particularly pyrolysis, have attracted significant attention in recent decades owing to their ability to recover valuable products, materials, and energy from waste tires [3].

Pyrolysis refers to a thermal decomposition process conducted in the absence of oxygen to convert macromolecular polymers into small-molecular compounds [4]. It provides a sustainable strategy for waste tire management by recovering reusable and recyclable products, including tire pyrolysis oil (TPO), pyrolysis gas, and pyrolysis carbon black (PCB). Numerous studies on the pyrolysis of waste tires and rubber materials have been reported and comprehensively reviewed, addressing various aspects such as feedstock characteristics, product composition, reactor configurations, operating conditions, pyrolysis kinetics, and decomposition mechanisms [5–9]. It has been well established that operating conditions, e.g., temperature, heating rate, particle size, carrier gas, and flow rate, etc., have a significant impact on the pyrolysis behavior, product distribution, and pollutant transformation. Among the pyrolysis products, limonene is a high-value product and consid-

†These authors contribute equally.

Correspondence to: Qiao Y Y, qiao_yingyun@126.com

Received: February 4, 2026; Revised: April 6, 2026; Accepted: April 25, 2026

ered a dominant component derived from tire pyrolysis. Previous study has summarized that its concentration in TPO can be substantial under optimized conditions, while the overall limonene yield on a tire basis is lower and depends strongly on reactor configuration and operating conditions [10]. In most conventional pyrolysis processes conducted under inert atmospheres with direct heating, the production of valuable chemicals is primarily regulated through optimization of operating conditions. However, such approaches often face limitations in selectively enhancing target compounds while simultaneously improving product quality.

Nevertheless, several emerging pyrolysis approaches, such as vacuum pyrolysis [11], microwave pyrolysis [12][13], pressurized pyrolysis [14], and photothermal pyrolysis [15][16], have been introduced for waste tire degradation to enhance liquid product yields and selectively produce target compounds. Silva et al. [16] systematically summarized the advantages and limitations of these pyrolysis approaches for tire conversion and concluded that the selection of an appropriate technique depends largely on the desired product yield and composition. Murena et al. [17] were among the first to investigate waste tire pyrolysis under a hydrogen atmosphere. Their results demonstrated improved depolymerization, lower molecular-weight TPO, and a higher degree of saturation in the products. However, their quantitative assessment was limited by analytical constraints associated with TPO characterization. Insights from fast pyrolysis conducted in hydrogen-containing carrier gases for coal, biomass, and other solid wastes indicate that hydrogen can enhance pyrolysis oil quality by reducing molecular weight and facilitating heteroatom removal[18–20]. Hydrogen-assisted fast pyrolysis is of particular interest because it combines the short vapor residence time of fast pyrolysis with the potential effects of hydrogen on reactive pyrolysis intermediates. Under these conditions, hydrogen may play a crucial role in thermal decomposition by promoting the cleavage of complex molecular structures and stabilizing reactive intermediates through hydrogenation. Despite these findings, studies focusing on waste tire decomposition under hydrogen or hydrogen-enriched atmospheres are still lacking. In particular, the influence of hydrogen on product yields, composition, and distribution has not yet been fully elucidated and therefore warrants further systematic investigation.

Sulfur is one of the challenging issues that limit the utilization and application of TPO. Sulfur-containing compounds primarily originate from the thermal decomposition of vulcanizing agents, accelerators, and anti-aging additives used during tire manufacturing [21]. Hu et al. [22] studied the migration of sulfur during the pyrolysis of waste tires and reported that more than half of the sulfur remained in the PCB, predominantly in the form of sulfate, inorganic sulfide, and thiophene. In the gaseous products, sulfur-containing species were mainly hydrogen sulfide, accompanied by minor amounts of sulfur dioxide, carbonyl sulfide, and mercaptans. Farooq et al. [23] further demonstrated, based on thermogravimetric analysis coupled with FTIR and MS (TG–FTIR–MS), that the release behavior of sulfur-containing gases is strongly influenced by heating rate. Qu et al. [24] identified thiophenes as the dominant sulfur-containing compounds in TPO, which can undergo secondary reactions to form benzothiophene, dibenzothiophene, and polycyclic thiophenes at lower heating rates. Similar to product composition and distribution, operating conditions exert a significant influence on sulfur distribution and transformation pathways. Previous studies have reported that the presence of hydrogen or oxygen in the reaction atmosphere can alter sulfur transformation behavior among pyrolysis products by promoting the cleavage of carbon–sulfur bonds [25]. Therefore, hydrogen-assisted fast pyrolysis may offer advantages not only in controlling product distribution and oil quality, but also in regulating sulfur migration during thermochemical conversion. However, the role of hydrogen in sulfur transformation during fast pyrolysis of waste tire has not been systematically investigated. Specifically, it remains unclear that impact of hydrogen on sulfur partitioning among gaseous, liquid, and solid products, as well as on the evolution of sulfur-containing species in TPO and PCB.

In this study, fast pyrolysis of waste tires was carried out in a laboratory-scale downdraft tubular reactor using varying hydrogen proportions in the carrier gas. The resulting products were systematically collected and characterized using multiple analytical techniques to enable both qualitative and quantitative evaluation. The D-Limonene and BTXs in TPO, as well as the hydrocarbon gases in the gaseous product, were further discussed. Furthermore, the effects of hydrogen on sulfur transformation behavior across different product phases were examined. The objective is to provide insights into hydrogen-assisted waste tire pyrolysis and its impact on product yield and composition, with particular emphasis on sulfur transformation.

2. Materials and methods

2.1. Materials

The source of waste tires (WT) used in this investigation was from a nearby waste recycling center (Qingdao, China), in the form of a mixture of smashed whole truck tires. The detailed physicochemical properties of the studied WT were reported and discussed in a previous study [26].

2.2. Fast pyrolysis via a downdraft tube reactor

Figure 1 illustrates the schematic diagram of the downdraft tubular reactor, which consists of a reaction system, carrier gas supply system, feeding system, and product collection system. A detailed description of the reactor design and its associated configurations have been reported elsewhere previously [19][27].

Prior to each experiment, the airtightness of the entire system was carefully examined to ensure proper sealing and reliable operation. The reactor was heated to the target temperature of 500°C using a surrounding resistance furnace at a heating rate of 10°C·min^{-1}, with a total flow rate of carrier gas at 150 mL·min^{-1}. The carrier gas is a mixture of nitrogen (99.999%) and hydrogen (99.999%) with hydrogen volumetric proportions of 0%, 5%, 10%, and 15%, respectively. Approximately 2.0 ± 0.1 g of waste tire sample was placed in a silicone tube designed for fast pyrolysis. Upon opening the spring clips, the sample rapidly entered the heated zone of the reactor, initiating fast pyrolysis under the prescribed experimental conditions. The pyrolysis process was sustained for 2 min to ensure complete devolatilization of the tire sample. After each experimental run, the resulting PCB was collected from the upper section of the reactor, while the pyrolysis gas was cap-

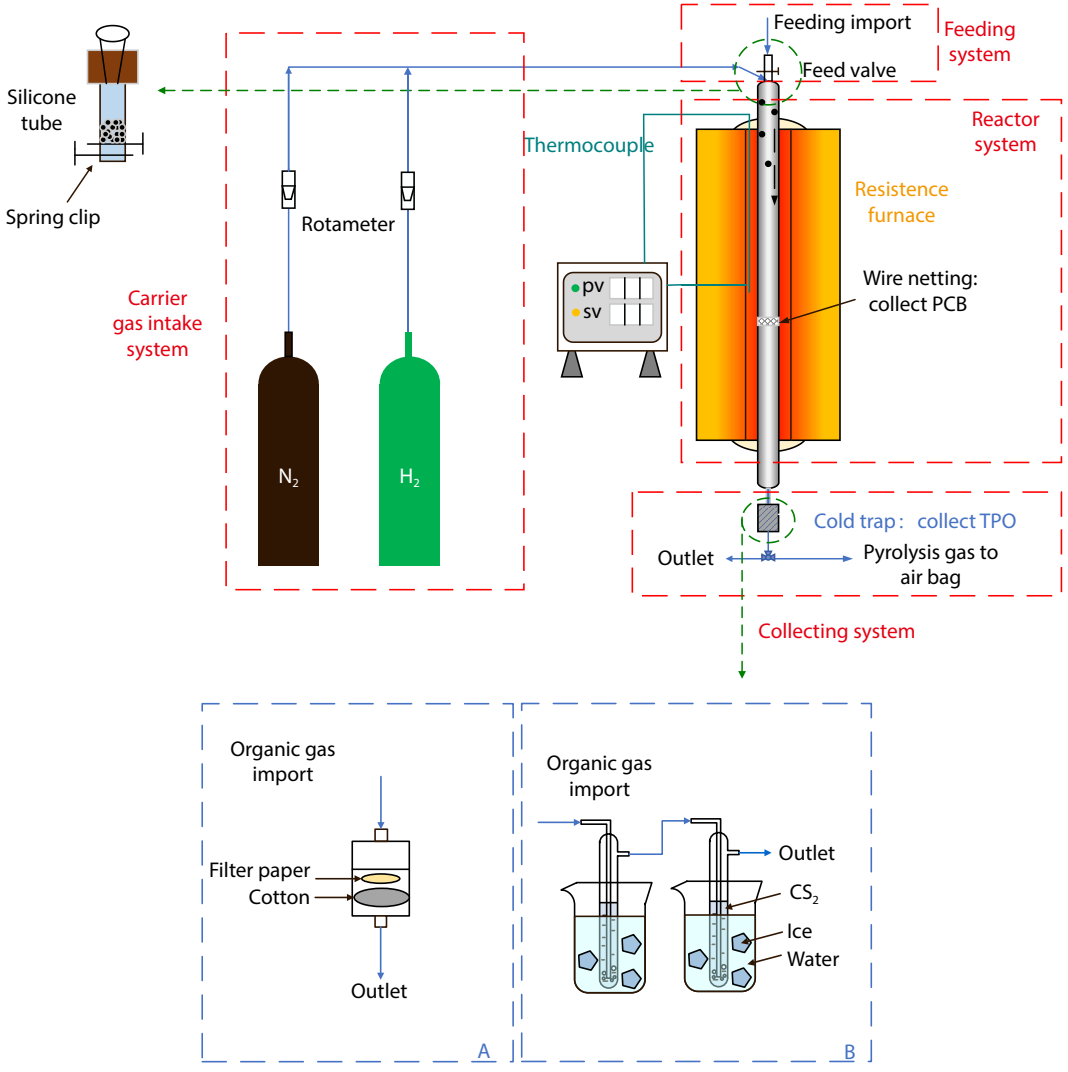

Fig. 1. Schematic diagram of the laboratory-scale downdraft tube reactor system with two different condensation modes.

tured using a gas collection bag.

Owing to the absorption of hydrogen sulfide (H_2S) by carbon disulfide (CS_2) in the pyrolysis gas and the subsequent volatilization of CS_2 during the experiment, accurate determination of TPO yield by direct mass difference measurement across the condensation system was not feasible. Consequently, all experiments were conducted using two distinct condensation modes to ensure reliable product analysis. Two types of condensation systems were employed in the experiments, as illustrated in **Figure 1**, and are hereafter referred to as Condensation A and Condensation B. Condensation A was used for the collection of pyrolysis gas and for determining the overall yield of TPO, whereas Condensation B was specifically designed to quantify the yields of D-limonene and BTX compounds present in the TPO. To ensure satisfactory repeatability and reproducibility, experiments incorporating different condensation systems were conducted four times, including three replicate runs using Condensation A and one run using Condensation B. Following the completion of each experimental run using Condensation A approach, the yields of TPO and PCB were determined gravimetrically based on the mass of the collected products as listed in Eq. (1) and (2). In contrast, the yield of gaseous products (Eq. (3)) was calculated by difference, because direct measurement of the gas mass was not practical under the present experimental conditions.

$$y_{TPO} = m_{TPO}/m_{Tire} \times 100\% \quad (1)$$

$$y_{PCB} = m_{PCB}/m_{Tire} \times 100\% \quad (2)$$

$$y_{Gas} = 100 - y_{TPO} - y_{PCB} \quad (3)$$

where y_{TPO}, y_{PCB}, and y_{Gas} represent the yields of pyrolysis products, and m_{TPO}, m_{PCB}, and m_{Tire} are the measured mass of TPO, PCB, and tire, respectively.2.3. Product characterization techniques

2.2.1. TPO analysis

The functional groups present in TPO were analyzed using attenuated total reflection–Fourier transform infrared spectroscopy (ATR–FTIR, Tensor II, Bruker). Prior to analysis, the diamond crystal was thoroughly cleaned with ethanol, and background spectra were collected and subtracted to eliminate interference. Residual liquid from Condensation A was gently wiped onto the crystal surface using absorbent cotton. Infrared spectra were recorded at a resolution of 4 cm^{-1} over the wavenumber range of 4000–440 cm^{-1}. The acquired spectra were baseline-corrected and normalized using OPUS soft-

ware (Version 7.5, Bruker). Detailed assignments of infrared absorption peaks and corresponding functional group vibrations are provided in Table S1 (Supplementary Material).

The analyses of compounds in TPO were conducted using gas chromatography–mass spectrometry (GC–MS, QP2010 SE, Shimadzu). High-purity helium (99.999%) was used as the carrier gas, and the injector temperature was set to 300°C. A 1 μL aliquot of the liquid mixture containing TPO and carbon disulfide (CS_2) collected from Condensation B was injected in split mode with a split ratio of 50:1. Chromatographic separation was achieved using a DB-5MS capillary column (60 m × 0.25 mm × 0.25 μm film thickness, Agilent). The detailed GC temperature program is summarized in Table S2 (Supplementary Material). The mass spectrometer was operated in full-scan mode over a mass-to-charge (m/z) range of 20–600 amu using electron ionization (EI) at 70 eV. To minimize the influence of CS_2 on the chromatographic peak areas of TPO components, a solvent delay of 400 s was applied to the total ion chromatogram. Compound identification was performed by comparing the obtained mass spectra with those in the NIST mass spectral library.

2.2.2. Pyrolysis gas analysis

The composition of pyrolysis gas was analyzed using gas chromatography (GC, SP-6890, Lunan-Ruihong Inc.) equipped with both a thermal conductivity detector (TCD) and a flame ionization detector (FID). The TCD was operated at 70°C for the detection of permanent gases, specifically N_2 and H_2, while hydrocarbon gases were analyzed using the FID under a programmed temperature regime. The temperature program for the FID was set as follows: (i) the oven temperature was held at 70°C for 3 min; (ii) it was ramped to 160°C at a heating rate of 5°C min^{-1}; and (iii) maintained at 160°C for 10 min. Because the pyrolysis gas derived from waste tires contained substantial amounts of hydrogen sulfide (H_2S) and other sulfur-containing compounds, an alkaline scrubbing pretreatment was applied before gas injection to prevent corrosion and damage to the GC system. As a consequence of this pretreatment and instrumental limitations, certain gaseous species, including CO, CO_2, and H_2S, could not be quantitatively detected in the present study.

The molar composition of the gaseous products obtained from GC analysis was converted to mass fractions using Eq. (4), and the yield of individual gas components was subsequently calculated according to Eq. (5):

$$W_f = C_f M_f / \Sigma C_f M_f \times 100 \quad (4)$$

$$Yiled_f = W_f \times y_{gas} \quad (5)$$

where W_f (wt.%) is the mass fraction of gas component f, C_f (mol%) is the corresponding molar fraction determined by GC analysis, M_f (g mol^{-1}) is the molar mass of the gas component, $Yield_f$ (g) represents the yield of the individual gas component, and y_{gas} (wt.%) denotes the total yield of pyrolysis gas.

2.2.3. Sulfur-containing compounds analysis

The concentration of H_2S in the pyrolysis gas was determined in accordance with the Chinese National Standard GB/T 11060.1–2010. The analytical principles and detailed experimental procedures are provided in the Supplementary Material. To minimize experimental uncertainty and ensure data reliability, all measurements were performed in triplicate.

The specific composition of sulfur-containing compounds in TPO was analyzed using gas chromatography–mass spectrometry (GC–MS) as mentioned above, with the relative abundance of individual species estimated based on chromatographic peak area normalization.

X-ray photoelectron spectroscopy (XPS, ESCALAB 250Xi, Thermo Fisher Scientific Inc.) was employed to characterize sulfur species on the surface of PCB. An Al Kα radiation source (hv = 1486.6 eV) was used at an operating power of 120 W. All spectra were calibrated against the C 1s peak at a binding energy of 284.8 eV to correct for surface charging effects.

3. Results and discussions

3.1. Product distribution

The yields of the three-phase products, including TPO, Gas, and PCB, under different hydrogen proportions are presented in **Figure 2**. The relatively small standard deviations shown in **Figure 2** suggest satisfactory repeatability of the hydrogen-assisted fast-pyrolysis experiments. The results show that the TPO yield increased slightly from 44.25 wt.% to 46.21 wt.% as the hydrogen content in the carrier gas increased to 5 vol.%. However, a further increase in hydrogen proportion led to a pronounced decrease in TPO yield, reaching 34.01 wt.% at the highest hydrogen proportion at 15 vol.%. In contrast, the yield of pyrolysis gas exhibited an opposite trend, which is shown as initially decreasing and subsequently increasing with increasing hydrogen proportions. In comparison with inert atmosphere pyrolysis, the presence of hydrogen promotes deeper decomposition and reforming of heavy fractions in the primary volatile vapors, which results in the enhanced formation of light gaseous products **[28]**. In addition, the existence of hydrogen would inactivate the free radicals at higher temperatures. The resultant hydrogen radical combines with the small molecule radicals in the volatile vapors to prevent further polymerization, thereby suppressing secondary polymerization reactions **[29]**. Consequently, the overall yield of TPO decreases with increasing hydrogen proportion during the fast pyrolysis of waste tires. The yield of PCB showed a slight decrease from 40.06 wt.% to 38.20 wt.% as the hydrogen proportion increased. It is attributed that the free radical fragments generated in the presence of hydrogen during pyrolysis are saturated and stabilized with the increment of hydrogen content. As hydrogen proportion increases, the formation of polymerization coke arising from macromolecular radical recombination

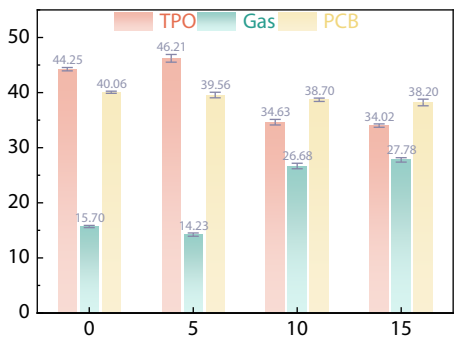

Fig. 2. The three-phase product yields under different hydrogen contents during fast pyrolysis of waste tires in the presence of hydrogen.

is inhibited, leading to a modest reduction in PCB yield.

The pyrolysis process of biomass and polymer generally involves the thermal decomposition of macromolecules to release volatile vapors, followed by the secondary reactions among these volatiles, e.g., secondary cracking, aromatization, isomerization, polycondensation and coking reaction, etc. **[30][31]**. In the presence of hydrogen during biomass pyrolysis, these secondary reactions can be significantly altered or intensified. For example, hydrogen has been reported to prolong the second decomposition stage of cellulose by promoting multiple reactions, including decarboxylation, hydrocracking, and hydrodeoxygenation **[32]**. A similar behavior can be inferred for the hydrogen-assisted pyrolysis of waste tires. As shown by the product distribution in **Figure 2**, the secondary reactions are evidently promoted when the hydrogen proportion in the carrier gas exceeds 5 vol.%. Increasing hydrogen concentration enhances the secondary cracking of high-molecular-weight volatile compounds, which leads to a decrease in TPO yield. Meanwhile, the polycondensation and coking reaction of volatiles are slightly inhibited in the presence of hydrogen radicals, resulting in a modest decline in PCB yield. From the perspective of product yield, fast pyrolysis of waste tires in the presence of H_2 leads to a slight increase in liquid yield at a relatively low hydrogen proportion (5 vol.%). However, with further increases in hydrogen concentration in the carrier gas, the production of gaseous products is markedly enhanced due to the intensified secondary hydrocracking of condensable volatile species.

3.2. Characteristics of TPO

3.2.1. FTIR analysis

The infrared spectra of the TPO measured under different hydrogen proportions are shown in **Figure 3**, and the detailed assignments of characteristic absorption bands and corresponding vibrational modes are summarized in Table S2 (Supplementary Material). It could be seen from Fig. 3 that the TPO is predominantly composed of aliphatic and aromatic hydrocarbons under all investigated conditions. Two strong absorption bands located at 2926 cm^{-1} and 2865 cm^{-1} are attributed to the $–CH_2–$ stretching vibration and $-CH_3$ stretching vibration, respectively. The bending vibration bands of $-CH_2$ and $-CH_3$ appear at 1454 cm^{-1} and 1376 cm^{-1} further confirm the presence of aliphatic hydrocarbons in TPO irrespective of hydrogen proportions. The C=C stretching vibration peak at 1647 cm^{-1} indicates the existence of olefinic compounds in TPO. This is further supported by the characteristic =C–H absorption peaks observed at 3072 cm^{-1}, 886 cm^{-1}, and 966 cm^{-1}. Aromatic compounds in TPO can be identified by the skeletal vibration bands at approximately 1600 cm^{-1} and 1510 cm^{-1}. Moreover, the aromatic C–H out-of-plane bending vibrations in the range of 700-850 cm^{-1} suggest the coexistence of aromatics with different substitution patterns. In addition to the characteristic absorption peaks of aliphatic and aromatic compounds, a C=O stretching vibration band is also found at 1707 cm^{-1}, which is likely associated with oxygen-containing compounds formed from the thermal decomposition of tire additives, such as carboxylic acids [33]. Overall, the FTIR analysis indicates that TPO produced under hydrogen-assisted pyrolysis conditions mainly consists of hydrocarbons and their oxygenated derivatives.

According to the Lambert–Beer law, the absorbance intensity of a given functional group is linearly proportional to the concentration of the corresponding chemical species [34]. Based on the FTIR spectra of TPO obtained under different hydrogen proportions, it can be preliminarily inferred that hydrogen exerts a measurable influence on the composition and chemical properties of TPO. In the absence of hydrogen in the carrier gas, the absorption bands associated with $–CH_2$ and $–CH_3$ functional groups are present but relatively weak, which indicates a lower degree of saturation in the resulting oil. With the introduction of hydrogen, a slight decrease in the intensity of the C=O stretching vibration is observed, which can be attributed to deoxygenation reactions, e.g., hydroxyalkylation of carbonyl groups, occur among volatile intermediates under hydrogen-assisted conditions [35]. In addition, the characteristic absorption bands of aromatic hydrocarbons, particularly the C–H out-of-plane bending vibrations in the range of 750–800 cm^{-1}, exhibit a noticeable increase in intensity at a hydrogen proportion of 5 vol.%, followed by a decline with further increases in hydrogen content. Nevertheless, despite the

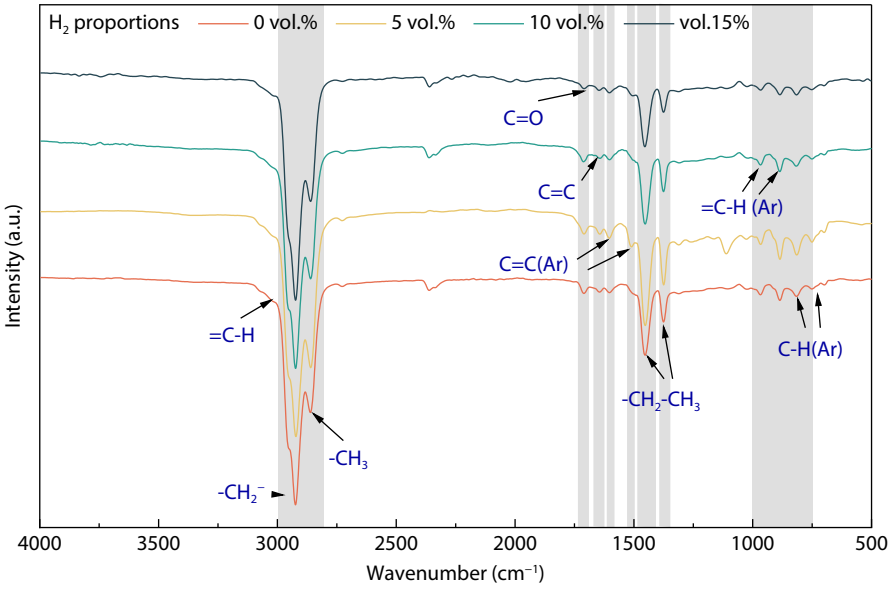

Fig. 3. FTIR spectra of TPO obtained during pyrolysis of waste tires in the presence of hydrogen.

non-monotonic variation in aromatic-related absorption bands, increasing the hydrogen proportion in the carrier gas leads to a generally higher saturation degree of compounds in TPO, as reflected by the FTIR functional group analysis.

3.2.2. GC/MS analysis

The total ion chromatograms (TICs) and detailed chemical compositions of TPO produced under different hydrogen proportions in the carrier gas are presented in Fig. S1 and Table S3 (Supplementary Material), respectively. The compounds identified in TPO derived from waste tire pyrolysis under hydrogen-enriched atmospheres can be classified into several categories based on their functional groups, including monoolefins, diolefins, triolefins, tetraolefins, cycloolefins, cyclodiolefins, cycloalkanes, sulfur-containing compounds, monoaromatic hydrocarbons (BTX), polycyclic aromatic hydrocarbons (PAHs), and other minor components such as nitrogen- and oxygen-containing compounds. Olefins constitute the dominant fraction of TPO, accounting for more than 60% of the total composition, with D-Limonene identified as the predominant olefinic compound. Aromatic hydrocarbons (around 15-25%) represent the second most abundant class of compounds, accompanied by a notable proportion of sulfur-containing species, accounting for approximately 3-4% of the total TPO composition. These results are consistent with previous studies, which have similarly reported olefins and aromatic hydrocarbons as the primary product classes generated during the pyrolysis of waste tires [36][37].

Figure 4 illustrates the distribution of compound classes in TPO and the variation in yields of representative products as a function of hydrogen proportion in the carrier gas. As shown in Figure 4(a), diolefins constitute the dominant product class, with their relative content increasing markedly from approximately 40% to 60% as the hydrogen proportion rises to 10 vol.%, followed by a slight further increase at 15 vol.% hydrogen. In contrast, the relative contents of monoolefins and triolefins decrease in the presence of hydrogen and remain relatively stable across different hydrogen proportions. In addition, tetraolefins are detected only when hydrogen is exited in the pyrolysis atmosphere, which indicates that hydrogen facilitates the formation of higher unsaturated olefin species. These results suggest that the presence of hydrogen during pyrolysis enhances olefin formation, particularly diolefins. Previous studies have reported slight hydrogenation of unsaturated hydrocarbons during polymer pyrolysis when hydrogen is used as a carrier gas [38]. However, under partial hydropyrolysis conditions employed in this study, the relatively low hydrogen concentration does not adversely affect olefin production. Instead, an increase in cycloalkane content is observed, which can be attributed to the hydrogenation of cycloolefins in the presence of hydrogen. Notably, the relative content of aromatic hydrocarbons decreases significantly, which suggests the suppression of aromatic formation in the presence of hydrogen. Furthermore, hydrogen promotes desulfurization and deoxygenation reactions that lead to reduced contents of sulfur- and oxygen-containing compounds, as shown in Figure 4(a). The similarity in product distributions observed at hydrogen proportions of 10 vol.% and 15 vol.% suggests that the system approaches a hydrogen-saturated state, beyond which excess hydrogen does not further participate in secondary reactions of volatile intermediates during waste tire pyrolysis.

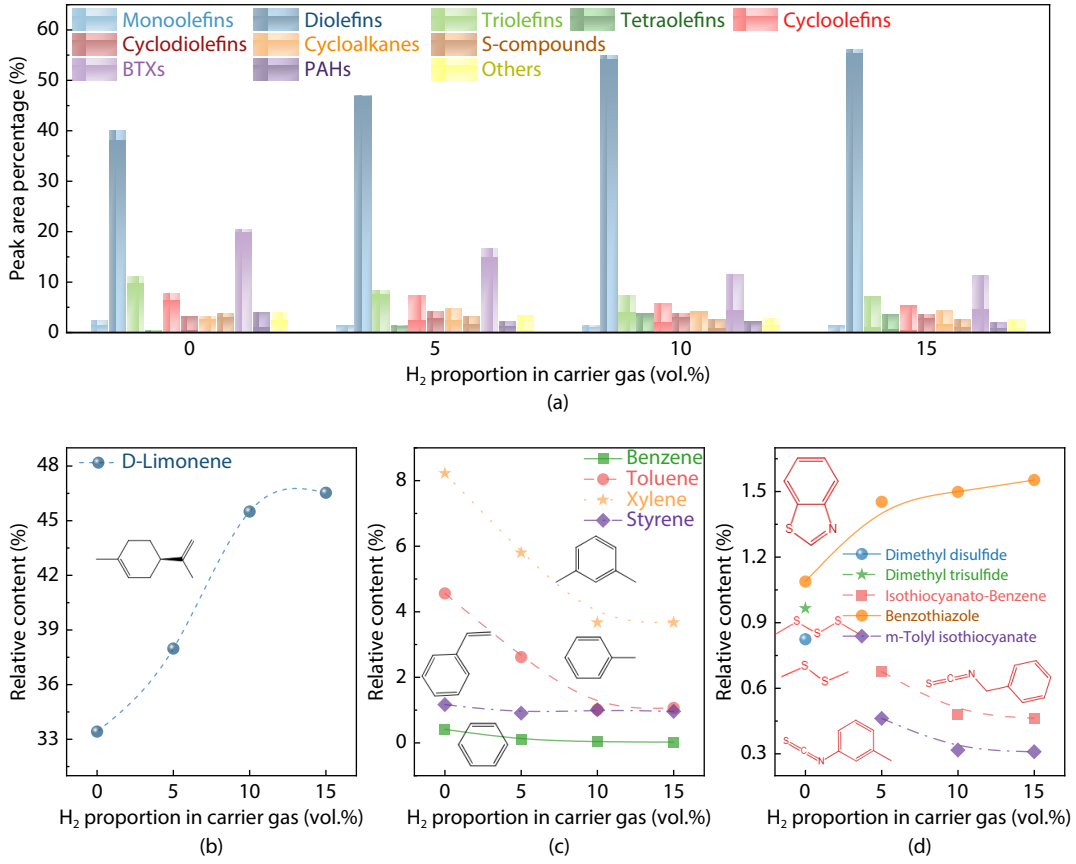

Fig. 4. GC/MS analysis of TPO during pyrolysis of waste tire in the presence of hydrogen, including product distribution under different hydrogen proportions in carrier gas (a) and the effects on the formation of D-Limonene (b), BTXs (c), and S-compounds (d).

The relative content of D-Limonene, the major diolefin (cyclic monoterpene), increases substantially with increasing hydrogen proportions, rising from 33.42% to 46.53%, as shown in Figure 4(b). Correspondingly, the contents of typical aromatic hydrocarbons, i.e., benzene, toluene, xylene, and styrene (Figure 4(c)), decrease significantly when the hydrogen is present in the pyrolysis environments. Compared with nitrogen, hydrogen is more chemically reactive and can generate hydrogen radicals that actively participate in secondary reactions during pyrolysis [39]. The formation of D-Limonene during tire pyrolysis is generally attributed to intramolecular cyclization of intermediate species or Diels-Alder reaction among short-chain diolefins [4][10]. The presence of hydrogen could hydrogenate unsaturated intermediates into the precursors, e.g., allylic radicals, thereby promoting D-Limonene formation. Apart from that, the hydrogen-containing environment also suppresses the cyclization, aromatization, and dehydrogenation that are necessary for monoaromatic hydrocarbons formation to some extent, resulting in less aromatics in TPO. The results suggest that the presence of hydrogen in carrier gas during tire pyrolysis enhances the formation of D-Limonene while inhibiting the formation of BTXs due to partial hydrogenation reactions of intermediate and suppression of aromatization pathways.

Figure 4(d) presents the effects of hydrogen on S-compounds in TPO. The relative content of benzothiazole increases from 1.08% to 1.55% along with the increased hydrogen proportions. The chain sulfides, dimethyl disulfide (0.88%) and dimethyl trisulfide (0.96%), are observed during conventional tire pyrolysis, whereas the type of sulfur-containing compounds is transformed into hydrogen-assisted pyrolysis. The results indicate that chain sulfides are almost completely converted into cyclic sulfides during pyrolysis, while the presence of hydrogen promotes the formation of benzothiazole. The detailed mechanisms regarding sulfur migration and distribution during the pyrolysis of waste tires in the presence of hydrogen will be discussed in the following.

3.3. Characteristics of pyrolysis gaseous product

The composition of pyrolysis gas produced during waste tire pyrolysis under different hydrogen proportions is summarized in **Table 1**. As discussed previously, the overall yield of pyrolysis gas increases markedly with increasing hydrogen content, rising from 15.70 wt.% in the absence of hydrogen to 27.78 wt.% at a hydrogen proportion of 15 vol.%. This enhancement in gas production is attributed to intensified secondary hydrocracking reactions among volatile vapors, which become particularly pronounced at hydrogen proportions of 10 vol.% and 15 vol.%.

Compared with the pyrolysis conducted under an inert atmosphere, the yields of H_2, CH_4, and other light hydrocarbons (C_nH_m) all increase in the presence of hydrogen. In general, the formation of CH_4 occurs through two primary pathways: (i) recombination of methyl radicals with hydrogen radicals and (ii) thermal cracking of macromolecular hydrocarbons [40]. The introduction of hydrogen promotes both pathways by supplying additional reactive hydrogen radicals. Similarly, the yields of other low-molecular-weight hydrocarbons (e.g., C_2H_4, C_2H_6, C_3H_6, C_3H_8) exhibit an increasing trend with increasing hydrogen proportion. The formation mechanisms of these hydrocarbons are analogous to those of CH_4, which involves the recombination of small hydrocarbon radicals, such as dimethyl, ethyl, and propyl radicals, with hydrogen radicals in the reaction zone.

Nevertheless, the relatively low hydrogen concentration in the carrier gas does not substantially alter the overall gas composition, as only minor variations are observed in **Table 1** when compared with pyrolysis under a nitrogen atmosphere, except for hydrogen (H_2) content. This behavior can be attributed to the preferential participation of hydrogen in reactions associated with TPO formation, which consume hydrogen before it significantly influences gas-phase composition. In addition, similar hydrocarbon gas compositions observed at hydrogen proportions of 10 vol.% and 15 vol.% indicate the presence of a threshold effect, beyond which further increases in hydrogen availability exert a limited impact on gas composition. Overall, the increased presence of hydrogen in the carrier gas primarily enhances secondary hydrocracking of heavy hydrocarbons and radical-mediated reactions among small molecular fragments. This results in elevated yields of gaseous products and light hydrocarbon gases, rather than significant changes in gas composition.

3.4. Sulfur transformation behaviors

3.4.1. Sulfur transformation behavior in gaseous products

Sulfur-containing gases generated during waste tire pyrolysis mainly include hydrogen sulfide (H_2S), sulfur dioxide (SO_2), car-

Table 1. Pyrolysis gas composition during waste tire pyrolysis at different hydrogen proportions.

Hydrogen proportion (vol.%)	0 vol.%	5 vol.%	10 vol.%	15 vol.%
Gaseous product yield (wt.%)	15.70	14.23	26.67	27.78
Gas composition (%)				
CH_4	1.50	1.68	3.18	3.63
C_2H_6	0.82	0.89	1.91	2.07
C_2H_4	1.63	1.96	2.91	3.37
C_3H_8	1.17	0.86	1.63	1.63
C_3H_6	2.13	2.12	3.55	4.06
C_4H_{10}	0.72	0.46	0.78	0.75
C_4H_8	7.36	4.50	8.92	9.36
C_5H_{12}	0.17	0.10	0.43	0.40
H_2	0.20	1.68	3.36	2.51
	Hydrogen sulfide (H_2S) content (wt.%)			
	1.32	1.53	5.09	5.31

bonyl sulfide (COS), and methyl mercaptan (CH_3SH). In most cases, H_2S constitutes approximately 85-95% of the total sulfur-containing gases, depending on the experimental conditions and tire sources, and can therefore be regarded as the representative sulfur species during pyrolysis [22][41]. Accordingly, in the present study, sulfur-containing gases were evaluated by quantifying the H_2S content in the pyrolysis gaseous product, as the representative gaseous product. As shown in **Table 1**, the H_2S content increased markedly from 1.32 wt.% to 5.31 wt.% with increasing hydrogen proportion in the carrier gas. This observation indicates that the presence of hydrogen in carrier gas promotes sulfur conversion toward H_2S rather than its retention in complex hydrocarbon structures [42]. The general formation pathways of H_2S during tire pyrolysis include (i) cleavage of C–S–C or C–S–S–C bonds to generate sulfur-centered radicals (C–S •), (ii) hydrogen abstraction leading to the formation of thiol intermediates (C–SH), and (iii) further cracking to yield •SH, which subsequently undergo hydrogenation with hydrogen radicals to form gaseous H_2S, as described by Eqs. (6–8) [23][43].

$$R_1 - S - R_2 \rightarrow R_1 - S\cdot + R_2 \xrightarrow{\cdot H} R_1 - SH + R_2 - H \quad (6)$$

$$R_1 - S - S - R_2 \rightarrow R_1 - S\cdot + R_2 - S \xrightarrow{\cdot H} R_1 - SH + R_2 - SH \quad (7)$$

$$R - SH \rightarrow R\cdot + \cdot SH \xrightarrow{\cdot H} R - H + H_2S \quad (8)$$

In addition, the •SH intermediate radicals may also react with hydroxyl radicals to form SO_2 or carbonyl species to produce COS. However, the distribution of sulfur-containing gaseous products strongly depends on the relative reactivity of available radicals. Among these, hydrogen radicals exhibit the highest reactivity, favoring hydrogenation pathways and resulting in H_2S as the dominant sulfur-containing gas under hydrogen-assisted pyrolysis conditions [25]. The formation mechanisms of sulfur gases, particularly H_2S, in the presence of hydrogen differ substantially from those occurring under inert atmospheres. On the one hand, sulfur-centered radicals generated during pyrolysis can rapidly react with hydrogen to form thermodynamically stable H_2S, rather than recombining to produce organic sulfur compounds [44]. On the other hand, the existence of hydrogen radicals enhances the scission of organic sulfur chains, leading to the generation of additional •SH radicals, which subsequently undergo hydrogenation to form H_2S. Through these pathways, hydrogen not only facilitates the conversion of sulfur into gaseous products but also suppresses the retention of sulfur in organic forms within condensed phases. This dual effect explains the enhanced sulfur release and increased H_2S formation observed during waste tire pyrolysis in the presence of hydrogen in pyrolysis atmospheres.

3.4.2. Sulfur transformation behavior in TPO

The relative peak area percentages of sulfur-containing compounds and representative sulfur species in TPO, as determined by GC–MS analysis, are presented in Figure 4(a) and Figure 4(d), respectively. It could be observed that the overall relative content of sulfur-containing compounds in TPO decreases progressively with increasing hydrogen proportion in the carrier gas, from 3.61% to 2.61%. This reduction can be attributed to the enhanced transformation of organic sulfur species into gaseous sulfur compounds in the presence of hydrogen. As discussed previously, reactive hydrogen species promote the cleavage of carbon–sulfur bonds in high-molecular-weight compounds, facilitating sulfur release into the gas phase and thereby reducing the abundance of sulfur-containing compounds in the liquid phase.

The main sulfur-containing compounds identified in TPO are m-Tolyl isothiocyanate, benzothiazole, isothiocyanato-benzene, dimethyl disulfide, and trisulfide dimethyl, as shown in Figure 4(d)). Among these species, benzothiazole is the dominant sulfur-containing compound in TPO. It is primarily derived from the thermal decomposition of vulcanization accelerators, such as thiazoles and sulfonamides, which are commonly added during tire manufacturing [45]. The content of benzothiazole is strongly influenced by the hydrogen proportion in the carrier gas, increasing markedly from 1.09% under an inert atmosphere to 1.45% at 5 vol.% hydrogen, followed by a gradual increase with further hydrogen addition, as shown in Figure 4(c). This trend suggests that hydrogen promotes the decomposition of vulcanization accelerators during the pyrolysis of waste tires in the presence of hydrogen [46]. In contrast, low-molecular-weight chain thioethers are detected only under inert pyrolysis conditions, which indicates that their formation is suppressed by the effect of hydrogen in atmosphere. Similar behavior has been reported for coal pyrolysis, where chain thioethers and sulfides are rarely observed under hydrogen atmospheres [42]. In addition, sulfur–cyanide compounds are formed in the presence of hydrogen, but their relative content decreases gradually as the hydrogen proportion increases that suggests further transformation of these intermediates under hydrogen-assisted conditions.

Figure 5 illustrates the proposed pathways for sulfur transformation in liquid organic compounds during the hydropyrolysis of waste tires, using the typical vulcanization accelerator 2-mercaptobenzothiazole (MBT) as a representative example. The initial stage b of sulfur transformation involves cleavage of the S-H bond in the mercapto group, leading to the formation of thiyl radicals, such as •SH, CH_3–S•, and R–S•. These sulfur-containing radicals can further react against to form benzothiazole, DMDS, DMTS, and small amounts of thiophenol, as well as releasing H_2S that comes from the hydrogen abstraction of •SH reaction [21]. The intermediate sulfur radicals may also interact to form thioethers, e.g., DMDS can be produced through the combination of methanethiol (CH_3–SH) and sulfur radicals (S•). However, DMDS and DMTS are not thermally stable compounds and are decomposed into various sulfur radicals, especially in the presence of hydrogen during pyrolysis. The decomposition is initiated by homolytic cleavage of S–C and S–S bonds to form additional reactive sulfur radicals [47]. These sulfur radicals and hydrogen radicals can recombine through radical addition, hydrogen abstractions, and sulfur homolytic substitutions to form higher-molecular-weight sulfur-containing molecules, i.e., isothiocyanato-benzene and m-Tolyl isothiocyanate. With the increasing hydrogen proportions in atmosphere, hydrogenation and cyclization reactions could possibly occur to convert some sulfur-cyanide intermediates into benzothiazole. This mechanism is consistent with the observed decrease in sulfur–cyanide compound concentra-

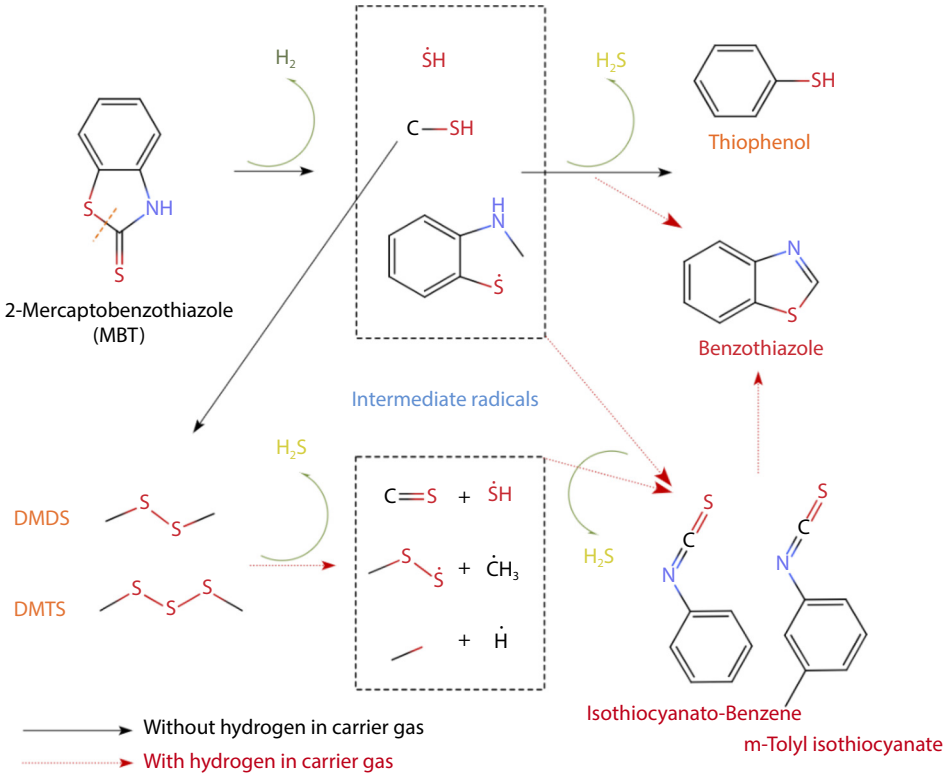

Fig. 5. Possible pathways for the sulfur transformation in TPO during pyrolysis of waste tires in the presence of hydrogen.

tion at higher hydrogen proportions. In addition, the sulfur radicals, e.g., •SH and •S–R, can also interact with the hydrocarbon radicals, e.g., $\bullet C_2H_3$ and $\bullet C_4H_6$, to form sulfur-containing heterocycle compounds [24]. Nevertheless, these species represent only minor components during the hydropyrolysis of waste tires. Overall, hydrogen in the carrier gas plays a critical role in stabilizing sulfur-centered intermediates and promoting the formation of benzothiazole and H_2S, while simultaneously reducing the overall concentration of sulfur-containing compounds in the liquid phase. This mechanistic framework provides a rational explanation for the observed sulfur redistribution during waste tire pyrolysis in the presence of hydrogen.

3.4.3. Sulfur transformation behavior in PCB

The chemical states of sulfur in PCB were analyzed using X-ray photoelectron spectroscopy (XPS), and the full survey spectrum is presented in Figure S2 (Supplementary Material). In the XPS spectra, the x-axis represents the electron binding energy, while the y-axis corresponds to the photoelectron intensity. The relative contents of surface functional groups were determined based on the integrated peak area ratios. The high-resolution S 2p spectra of sulfur species remaining in the solid residues are shown in **Figure 6**. Sulfur in PCB can be classified into four chemical forms according to their characteristic binding energies, including inorganic sulfide (162.2 eV), thiol (163.6 eV), thiophenic sulfur (165.3 eV), and sulfate (170.1 eV). The assignment of these sulfur species is consistent with previously reported studies, with minor discrepancies likely arising from differences in tire feedstock composition and operating conditions [41][48]. Among these species, inorganic sulfide and sulfate are categorized as inorganic sulfur, whereas thiol and thiophenic sulfur are considered as organic sulfur. The results indicate that inorganic sulfide and thiol are the predominant sulfur species present in PCB during waste tire pyrolysis in the presence of hydrogen. This distribution suggests that hydrogen-assisted pyrolysis influences sulfur speciation in the solid phase, favoring the retention of reduced sulfur forms while promoting the migration of other sulfur species to gaseous and liquid products.

The relative proportions of different sulfur species in PCB are summarized in Table 2. For the organic sulfur species, thiophenic sulfur increases continuously from 10.63% to 13.88% with increasing hydrogen proportion. By contrast, thiol sulfur remains the major component and shows an overall decrease from 42.94% to 40.83%. An increase in hydrogen content promotes the decomposition of organic sulfides, leading to the generation of •SH radicals and the subsequent release of H_2S. Meanwhile, the interactions between •SH radicals and ash-forming elements retention in char (e.g., Ca, Zn, Fe, etc.) can immobilize sulfur in solid residues in the form of inorganic sulfides or sulfates, as described by Eq. 9 and Eq. 10 [22].

$$MO + \cdot SH \longrightarrow MS + \cdot OH \tag{9}$$

$$MO + \cdot SH + 3 \cdot OH \longrightarrow MSO_4 + 2H_2 \tag{10}$$

The decrease in the percentage of inorganic sulfides, from 39.42% to 36.73%, indicates that hydrogen suppresses the retention of sulfur in sulfide form within the solid residue. This behavior may be associated with the hydrogen-assisted stabilization of sulfur-containing radicals and the enhanced formation of volatile sulfur species such as H_2S, thereby reducing the probability of sulfur fixation as metal sulfides in char. Moreover, hydrogen may also modify the char surface that weakens the interactions among radicals and solid matrix to reduce the possibility of inorganic sulfides formation [49]. In contrast, the interactions between sulfur radicals and metal species in the char are enhanced in the presence of hydrogen, promoting the formation of sulfates. This effect can be attributed to

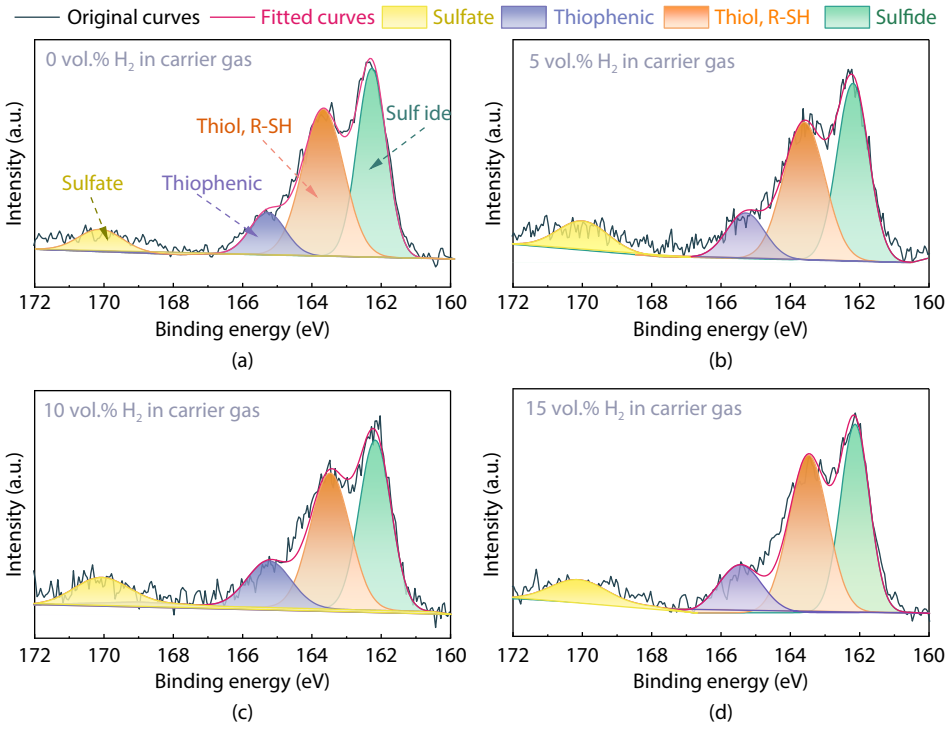

Fig. 6. XPS spectra of S 2p for PCB during waste tire pyrolysis at different hydrogen proportions of 0 vol.% (a), 5 vol.% (b), 10 vol.% (c), and 15 vol.% (d).

Table 2. Normalized peak area and relative area percentage of sulfur species in PCB based on XPS results.

Binding Energy (eV)		H_2 proportions (vol.%)			
		0	5	10	15
Inorganic Sulfide (162.2eV)	Peak area	2277.60	1240.32	1056.43	1116.34
	Area percentage	39.42%	38.89%	37.91%	36.73%
Thiol, R-SH (163.6eV)	Peak area	2477.75	1245.13	1105.01	1241.12
	Area percentage	42.94%	39.04%	39.65%	40.83%
Thiophenic (165.3eV)	Peak area	613.68	380.43	360.86	422.07
	Area percentage	10.63%	11.92%	12.95%	13.88%
Sulfate (170.1eV)	Peak area	401.09	323.39	264.34	259.65
	Area percentage	6.98%	10.14%	9.49%	8.54%

the increased reactivity of ash-forming elements (e.g., Ca, Zn, and Fe) activated by hydrogen. Besides, the proportion of sulfate increases significantly from 6.98% in the absence of hydrogen to 10.14% at 5 vol.% H_2, and then slightly decreases to 9.49% and 8.54% at 10 and 15 vol.% H_2, respectively. It might be attributed to the decomposition of organic sulfur compounds into sulfates. The presence of hydrogen can destabilize the C–S bonds in thiophenic structures through hydrogenation or radical addition, leading to ring opening and subsequent decomposition into olefins, sulfur compounds, and H_2S [50]. However, the reaction rates of thiophene desulfurization and hydrogenation depend on the equilibrium of •S radicals and H_2S-H_2 gas mixture, which means high hydrogen proportion might not be favorable for further decomposition [51]. In general, the role of hydrogen during pyrolysis could redistribute sulfur among different surface species, with a particularly pronounced increase in sulfate formation in solid residues.

3.5. Decomposition and sulfur transformation mechanism

A simplified reaction scheme is proposed to illustrate waste tire pyrolysis in the presence of hydrogen based on the provided product compositional results. The primary elastomer constituents (i.e., natural rubber, styrene-butadiene rubber, and butadiene rubber) undergo cleavage of C–C, C–S, and S–S bonds to form macroradicals, low-molecular-weight olefins, and intermediates. These intermediates mainly undergo secondary cracking, cyclization, aromatization, and polycondensation to generate liquid (TPO), gaseous (gas), and solid (PCB) products under an inert atmosphere. In the presence of H_2 in the atmosphere, hydrogen addition can stabilize radical fragments, promote the hydrogenation of unsaturated species, and inhibit excessive radical recombination and condensation. The product distribution is affected by the addition of hydrogen during waste tire pyrolysis.

Moreover, the possible transformation pathways of sulfur during waste tire pyrolysis under a partial hydrogen atmosphere are also proposed and illustrated in **Figure 7**. In the presence of hydrogen, the formation and transformation of sulfur-containing species proceed through several key stages, including (i) cleavage of sulfur-containing bonds in monomers or intermediate compounds during the initial pyrolysis stage; (ii) com-

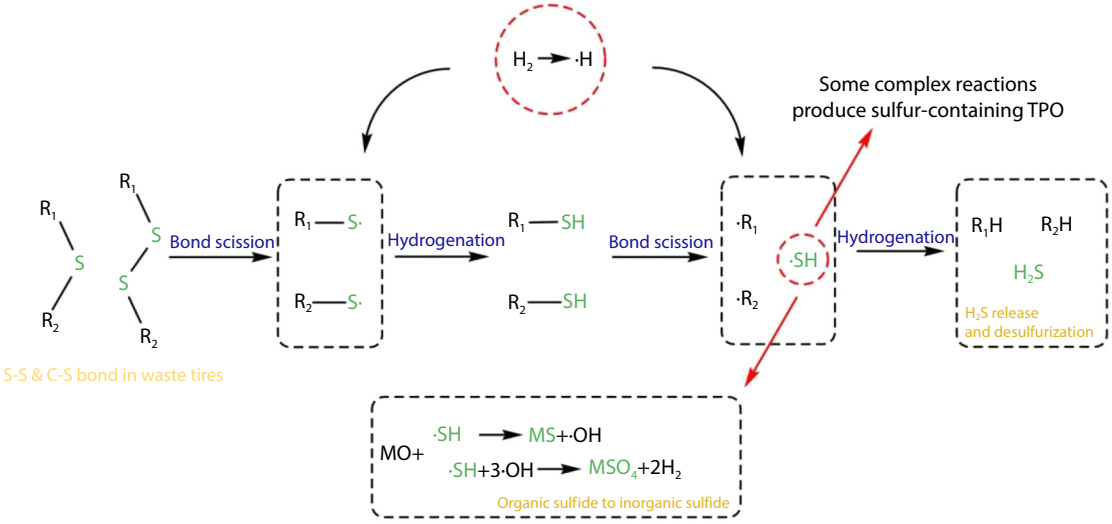

Fig. 7. The possible migration pathways of sulfur during pyrolysis of waste tires in the presence of hydrogen.

plex radical-mediated reactions among the generated intermediates, including hydrogenation, bond cleavage, reverse recombination, hydrogen abstraction, addition, and substitution reactions; and (iii) desulfurization and sulfur redistribution among the products through interactions involving sulfur-centered radicals. The presence of hydrogen markedly promotes sulfur migration into the gaseous phase in the form of hydrogen sulfide (H_2S) by enhancing hydrogenation reactions involving sulfur-hydrogen radicals (•SH). Consequently, the concentration of sulfur-containing compounds in the liquid phase is reduced, while thioethers are progressively transformed into sulfur–cyanide compounds under hydrogen-assisted conditions. In addition, hydrogen facilitates the conversion of organic sulfur into inorganic sulfur species in the solid residues to a certain extent, thereby influencing sulfur partitioning across the gas, liquid, and solid phases during waste tire pyrolysis.

4. Conclusion

The effects of hydrogen proportion on product distribution and sulfur transformation during waste tire pyrolysis were systematically investigated using a laboratory-scale downdraft tube reactor. Compared with inert-atmosphere pyrolysis, increasing the hydrogen proportion in the carrier gas significantly enhanced the yield of pyrolysis gas, while the yields of TPO and PCB decreased overall due to intensified secondary hydrocracking reactions. Hydrogen markedly influenced product composition by promoting the formation of D-limonene through hydrogenation of unsaturated intermediates and suppressing the formation of aromatic hydrocarbons, particularly BTX compounds. Meanwhile, the release of light hydrocarbon gases increased because of enhanced cracking of heavy volatile species. Similar compositions of TPO and gaseous products observed at hydrogen proportions of 10 vol.% and 15 vol.% indicate that the system approached a hydrogen-saturated regime, beyond which additional hydrogen exerted limited effects. Regarding sulfur behavior, hydrogen facilitated sulfur bond cleavage and stabilized sulfur-centered radicals that lead to increased H_2S release, especially at hydrogen proportions above 10 vol.%. Benzothiazole was identified as the dominant sulfur-containing compound in TPO, with its formation promoted under the effect of hydrogen in atmosphere. In the solid phase, hydrogen enhanced the transformation of organic sulfur into inorganic sulfur species within PCB. Overall, hydrogen plays a critical role in regulating product distribution, enhancing desulfurization, and controlling sulfur migration during waste tire pyrolysis.

Acknowledgments

The authors gratefully acknowledge the funding supported by the Shandong Provincial Natural Science Foundation (Major Basic Research Project, No.: ZR2024ZD33), Taishan Scholar Distinguished Professor Program (No.: tstp20240505), Taishan Scholar Specialized Team Program (No.: tstp20231217), and Excellent Youth Team Fund of China University of Petroleum (East China) (No.: 23CX10005A).

Conflicts of Interest

The authors declare that there are no conflicts of interest in this work.

Data Availability

All data needed to support the conclusions in the paper are presented in the manuscript and/or the Supplementary Materials. Additional data related to this paper may be requested from the corresponding author upon request.

Electronic Supplementary Material (ESM)

The online version contains supplementary material available at https://doi.org/10.26599/ECS.2026.9600030.

References

[1] Rogachuk, B. E., Okolie, J. A. Waste tires based biorefinery for biofuels and value-added materials production. *Chem. Eng. J. Adv.*, 2023, 14: 100476.

[2] Czajczyńska, D.; Krzyżyńska, R.; Jouhara, H.; Spencer, N. Use of pyrolytic gas from waste tire as a fuel: A review. *Energy*, 2017, 134: 1121–1131.

[3] Hita, I.; Arabiourrutia, M.; Olazar, M.; Bilbao, J.; Arandes, J. M., Castaño, P. Opportunities and barriers for producing high quality fuels from the pyrolysis of scrap tires. *Renew. Sustain. Energy Rev.*, 2016, 56: 745–759.

[4] Xu, F. F.; Wang, B.; Yang, D.; Ming, X.; Jiang, Y.; Hao, J. H.; Qiao, Y.

Y.; Tian, Y. Y. TG-FTIR and Py-GC/MS study on pyrolysis mechanism and products distribution of waste bicycle tire. *Energy Convers. Manag.*, 2018, 175: 288–297.

[5] Li, D.; Lei, S. J.; Lin, F. W.; Zhong, L.; Ma, W. C.; Chen, G. Y. Study of scrap tires pyrolysis–Products distribution and mechanism. *Energy*, 2020, 213: 119038.

[6] Ramírez Arias, A. M.; Moreno-Piraján, J. C.; Giraldo, L. Kinetic study of waste tire pyrolysis using thermogravimetric analysis. *ACS Omega*, 2022, 7: 16298–16305.

[7] Čepić, Z.; Mihajlović, V.; Đurić, S.; Milotić, M.; Stošić, M.; Stepanov, B.; Ilić Mićunović, M. Experimental analysis of temperature influence on waste tire pyrolysis. *Energies*, 2021, 14: 5403.

[8] Gauthier-Maradei, P.; Tavera Ruiz, C. P., Capron, M. Oil and aromatic yield maximization during pyrolysis of scrap tire rubber. *Waste Biomass Valorization*, 2019, 10: 3723–3733.

[9] Nisar, J.; Ali, G.; Ullah, N.; Ahmad Awan, I.; Iqbal, M.; Shah, A.; Sirajuddin, Sayed, M.; Mahmood, T.; Khan, M. S. Pyrolysis of waste tire rubber: Influence of temperature on pyrolysates yield. *J. Environ. Chem. Eng.*, 2018, 6: 3469–3473.

[10] Danon, B.; van der Gryp, P.; Schwarz, C. E., Görgens, J. F. A review of dipentene (dl-limonene) production from waste tire pyrolysis. *J. Anal. Appl. Pyrolysis*, 2015, 112: 1–13.

[11] Zhang, X. H.; Wang, T. J.; Ma, L. L.; Chang, J. Vacuum pyrolysis of waste tires with basic additives. *Waste Manag.*, 2008, 28: 2301–2310.

[12] Undri, A.; Rosi, L.; Frediani, M.; Frediani, P. Upgraded fuel from microwave assisted pyrolysis of waste tire. *Fuel*, 2014, 115: 600–608.

[13] Song, Z. L.; Liu, L.; Yang, Y. Q.; Sun, J.; Zhao, X. Q.; Wang, W. L.; Mao, Y. P.; Yuan, X. L.; Wang, Q. S. Characteristics of limonene formation during microwave pyrolysis of scrap tires and quantitative analysis. *Energy*, 2018, 142: 953–961.

[14] Ma, S. J.; Leong, H.; He, L. M.; Xiong, Z.; Han, H. D.; Jiang, L.; Wang, Y.; Hu, S.; Su, S.; Xiang, J. Effects of pressure and residence time on limonene production in waste tires pyrolysis process. *J. Anal. Appl. Pyrolysis*, 2020, 151: 104899.

[15] Ren, Q. Q.; Zhang, J. L.; Hu, S.; Ma, S. J.; Huang, R.; Su, S.; Wang, Y.; Jiang, L.; Xu, J.; Xiang, J. Novel photothermal pyrolysis on waste tire to generate high-yield limonene. *Fuel*, 2022, 329: 125482.

[16] Silva, W. O., Nagar, B.; Ellersiek, D.; Bondaz, L.; Espín, J.; Soutrenon, M.; Girault, H. H. Hydrogen production by waste tire recycling by photo-pyrolysis. *Sustainable Energy Fuels*, 2023, 7: 5693–5703.

[17] Murena, F.; Garufi, E.; Smith, R. B., Gioia, F. Hydrogenative pyrolysis of waste tires. *J. Hazard. Mater.*, 1996, 50: 79–98.

[18] Oh, S.; Lee, J.; Lam, S. S., Kwon, E. E., Ha, J. M.; Tsang, D. C. W., Ok, Y. S., Chen, W. H.; Park, Y. K. Fast hydropyrolysis of biomass Conversion: A comparative review. *Bioresour. Technol.*, 2021, 342: 126067.

[19] Tian, Y. Y.; Li, J.; Wei, W.; Zong, P. J.; Zhang, D.; Zhu, Y. N.; Qiao, Y. Y. Parametric effect of biomass partial hydropyrolysis process in a downer reactor to co-produce high-quality tar and syngas. *Bioresour. Technol.*, 2021, 320: 124401.

[20] Wang, J. X.; Cao, J. P.; Zhao, X. Y.; Liu, T. L.; Wei, F.; Fan, X.; Zhao, Y. P.; Wei, X. Y. Study on pine sawdust pyrolysis behavior by fast pyrolysis under inert and reductive atmospheres. *J. Anal. Appl. Pyrolysis*, 2017, 125: 279–288.

[21] Liu, S.; Yu, J.; Bikane, K.; Chen, T.; Ma, C.; Wang, B.; Sun, L. S. Rubber pyrolysis: Kinetic modeling and vulcanization effects. *Energy*, 2018, 155: 215–225.

[22] Hu, H. Y.; Fang, Y.; Liu, H.; Yu, R.; Luo, G. Q.; Liu, W. Q.; Li, A. J.; Yao, H. The fate of sulfur during rapid pyrolysis of scrap tires. *Chemosphere*, 2014, 97: 102–107.

[23] Farooq, M. Z., Yu, H. D.; Lin, F. W.; Rajput, M. I., Kumar, A.; Chen, G. Y. Kinetic insights and pollution mitigation in waste tire pyrolysis: Targeting sulfur, nitrogen, and PAHs emissions. *J. Anal. Appl. Pyrolysis*, 2024, 181: 106626.

[24] Qu, B. Y.; Liu, C. Q.; Zhang, Y. L.; Fu, Z. G.; Zhang, Y. S.; Li, A. M.; Ji, G. Z. Effect of heating rates on the fate of sulfur during waste tire pyrolysis. *Chem. Eng. J.*, 2023, 474: 145736.

[25] Zhang, W. J.; Cheng, Y. N.; Kong, J.; Wang, M. J.; Chang, L. P.; Bao, W. R. Effects of active hydrogen and oxygen on organic sulfur transformation behavior during pyrolysis of high sulfur coal: A review. *J. Fuel Chem. Technol.*, 2022, 50: 652–663.

[26] Xu, F. F.; Shao, Y. H.; Zhang, Y. P.; Zong, P. J.; Tian, Y. Y.; Wang, J. X.; Qiao, Y. Y. Parametric investigation of the effects on waste tire pyrolysis oil in a downdraft tube reactor. *Energy*, 2025, 314: 134267.

[27] Xu, F. F.; Ming, X.; Jia, R.; Zhao, M.; Wang, B.; Qiao, Y. Y.; Tian, Y. Y. Effects of operating parameters on products yield and volatiles composition during fast pyrolysis of food waste in the presence of hydrogen. *Fuel Process. Technol.*, 2020, 210: 106558.

[28] Meesuk, S.; Cao, J. P.; Sato, K.; Ogawa, Y.; Takarada, T. Fast pyrolysis of rice husk in a fluidized bed: Effects of the gas atmosphere and catalyst on bio-oil with a relatively low content of oxygen. *Energy Fuels*, 2011, 25: 4113–4121.

[29] Zhao, X. Y.; Ren, J.; Cao, J. P.; Wei, F.; Zhu, C.; Fan, X.; Zhao, Y. P.; Wei, X. Y. Catalytic reforming of volatiles from biomass pyrolysis for hydrogen-rich gas production over limonite ore. *Energy Fuels*, 2017, 31: 4054–4060.

[30] Chen, G. Y.; Farooq, M. Z., Sun, B. Y.; Lin, F. W.; Yan, B. B.; Rajput, G.; Chawla, M. Pollutants formation, distribution, and reaction mechanism during WT pyrolysis: A review. *J. Anal. Appl. Pyrolysis*, 2021, 157: 105218.

[31] Gautam, R.; Vinu, R. Unraveling the interactions in fast co-pyrolysis of microalgae model compounds *via* pyrolysis-GC/MS and pyrolysis-FTIR techniques. *React. Chem. Eng.*, 2019, 4: 278–297.

[32] Li, T.; Miao, K.; Zhao, Z. G.; Li, Y. Q.; Wang, H. Y.; Watanabe, A.; Teramae, N.; Wang, K. G. Understanding cellulose pyrolysis under hydrogen atmosphere. *Energy Convers. Manag.*, 2022, 254: 115195.

[33] Menares, T.; Herrera, J.; Romero, R.; Osorio, P.; Arteaga-Pérez, L. E. Waste tires pyrolysis kinetics and reaction mechanisms explained by TGA and Py-GC/MS under kinetically-controlled regime. *Waste Manag.*, 2020, 102: 21–29.

[34] Tian, B.; Qiao, Y. Y.; Bai, L.; Feng, W.; Jiang, Y.; Tian, Y. Y. Pyrolysis behavior and kinetics of the trapped small molecular phase in a lignite. *Energy Convers. Manag.*, 2017, 140: 109–120.

[35] Zhao, C.; Camaioni, D. M., Lercher, J. A. Selective catalytic hydroalkylation and deoxygenation of substituted phenols to bicycloalkanes. *J. Catal.*, 2012, 288: 92–103.

[36] Costa, G. A., dos Santos, R. G. Fractionation of tire pyrolysis oil into a light fuel fraction by steam distillation. *Fuel*, 2019, 241: 558–563.

[37] Choi, G. G.; Oh, S. J.; Kim, J. S. Non-catalytic pyrolysis of scrap tires using a newly developed two-stage pyrolyzer for the production of a pyrolysis oil with a low sulfur content. *Appl. Energy*, 2016, 170: 140–147.

[38] Watanabe, A.; Watanabe, C.; Freeman, R. R.; Teramae, N.; Ohtani, H. Hydrogenation reactions during pyrolysis-gas chromatography/mass spectrometry analysis of polymer samples using hydrogen carrier gas. *Anal. Chem.*, 2016, 88: 5462–5468.

[39] Abbas-Abadi, M. S., Haghighi, M. N., Yeganeh, H.; McDonald, A. G. Evaluation of pyrolysis process parameters on polypropylene degradation products. *J. Anal. Appl. Pyrolysis*, 2014, 109: 272–277.

[40] Yan, G. X.; Jing, X. D.; Wen, H.; Xiang, S. G. Thermal cracking of virgin and waste plastics of PP and LDPE in a semibatch reactor under atmospheric pressure. *Energy Fuels*, 2015, 29: 2289–2298.

[41] Wang, H.; Hu, H. Y.; Yang, Y. H.; Liu, H.; Tang, H.; Xu, S. H.; Li, A. J.; Yao, H. Effect of high heating rates on products distribution and sulfur transformation during the pyrolysis of waste tires. *Waste Manag.*, 2020, 118: 9–17.

[42] Gu, Y.; Yperman, J.; Vandewijngaarden, J.; Reggers, G.; Carleer, R. Organic and inorganic sulphur compounds releases from high-pyrite coal pyrolysis in H_2, N_2 and CO_2: Test case Chinese LZ coal. *Fuel*, 2017, 202: 494–502.

[43] Rahman, M. M., Yu, Y.; Wu, H. W. Valorisation of waste tyre *via* pyrolysis: Advances and perspectives. *Energy Fuels*, 2022, 36: 12429–12474.

[44] Zhou, Q.; Hu, H. Q.; Liu, Q. R.; Zhu, S. W.; Zhao, R. Effect of atmosphere on evolution of sulfur-containing gases during coal pyrolysis. *Energy Fuels*, 2005, 19: 892–897.

[45] Mkhize, N. M., Danon, B.; Alvarez, J.; Lopez, G.; Amutio, M.; Bilbao, J.; Olazar, M.; van der Gryp, P.; Görgens, J. F. Influence of reactor and condensation system design on tyre pyrolysis products yields. *J. Anal. Appl. Pyrolysis*, 2019, 143: 104683.

[46] Wang, B.; Fu, Y. F.; Zheng, H. B.; Zeng, D. W.; Xiao, R. Catalytic and noncatalytic fast pyrolysis of waste tires to produce high-value monocyclic aromatic hydrocarbons. *J. Anal. Appl. Pyrolysis*, 2021, 156: 105131.

[47] Vandeputte, A. G.; Reyniers, M. F.; Marin, G. B. Theoretical study of the thermal decomposition of dimethyl disulfide. *J. Phys. Chem. A*, 2010, 114: 10531–10549.

[48] Cao, C. Y.; Ren, Y.; Wang, H.; Hu, H. Y.; Yi, B. J.; Li, X.; Wang, L. L.; Yao, H. Insights into the role of CaO addition on the products distribution and sulfur transformation during simulated solar-powered pyrolysis of waste tires. *Fuel*, 2022, 314: 122795.

[49] Yan, J. D.; Yang, J. L.; Liu, Z. Y. SH radical: the key intermediate in sulfur transformation during thermal processing of coal. *Environ. Sci. Technol.*, 2005, 39: 5043–5051.

[50] Xian, S. X.; Xu, Q.; Li, H. W. Mechanism insight into the conversion between H_2S and thiophene during coal pyrolysis: A theoretical study. *ACS Omega*, 2023, 8: 33982–33996.

[51] Yik, E.; Hibbitts, D.; Wang, H. M.; Iglesia, E. Hydrogenation and CS bond activation pathways in thiophene and tetrahydrothiophene reactions on sulfur-passivated surfaces of Ru, Pt, and Re nanoparticles. *Appl. Catal. B Environ.*, 2021, 291: 119797.